Analytical Biochemistry **278,** 22–28 (2000)
doi:10.1006/abio.1999.4360, available online at http://www.idealibrary.com on IDEAL®

Direct Electrochemistry of Horseradish Peroxidase Immobilized on a Colloid/Cysteamine-Modified Gold Electrode

Xiao Yi, Ju Huang-Xian, and Chen Hong-Yuan[1]

Department of Chemistry, State Key Laboratory of Coordination Chemistry, Nanjing University, Nanjing 210093, People's Republic of China

Received July 26, 1999

Direct electron transfer of immobilized horseradish peroxidase on gold colloid and its application as a biosensor were investigated by using electrochemical methods. The Au colloids were associated with a cysteamine monolayer on the gold electrode surface. A pair of redox peaks attributed to the direct redox reaction of horseradish peroxidase (HRP) were observed at the HRP/Au colloid/cysteamine-modified electrode in 0.1 M phosphate buffer (pH 7.0). The surface coverage of HRP immobilized on Au colloid was about 7.6×10^{-10} mol/cm^2. The sensor displayed an excellent electrocatalytic response to the reduction of H_2O_2 without the aid of an electron mediator. The calibration range of H_2O_2 was 1.4 μM to 9.2 mM with good linear relation from 1.4 μM to 2.8 mM. A detection limit of 0.58 μM was estimated at a signal-to-noise ratio of 3. The sensor showed good reproducibility for the determination of H_2O_2. The variation coefficients were 3.1 and 3.9% (n = 10) at 46 μM and 2.8 mM H_2O_2, respectively. The response showed a Michaelis–Menten behavior at higher H_2O_2 concentrations. The K_M^{app} value for the H_2O_2 sensor was found to be 2.3 mM.

Key Words: **horseradish peroxidase; direct electrochemistry; Au colloid; cysteamine; biosensor, self-assembled monolayers.**

Heterogeneous electron-transfer (eT)[2] reaction of redox proteins has been widely investigated at various electrodes to elucidate the complex mechanisms of biological eT and determine their potential application in biotechnology (1, 2). It is known that the electroactive cofactors of all redox enzymes are bound in the enzyme structure and buried inside the insulated protein shells. In general, the direct eT behavior of redox enzyme between the cofactor and electrode is complicated due to the consequent structural degradation of protein resulting from its adsorption on the bulk electrode surface and/or the steric hindrance of the insulated shell of the immobilized protein. The eT has been facilitated on the electrode surface by using a soluble electron mediator in solution (3) or in immobilized layer (4, 5), where the mediator can diffuse from the cofactor to the electrode and vice versa.

Horseradish peroxidase (HRP), as an example, has been intensively used for the construction of amperometric biosensors for the determination of H_2O_2 and small organic peroxides and for the sensing of glucose, alcohol, and amino acids by coimmobilization of the corresponding oxidase on the same electrode surface (6). The direct eT of immobilized HRP, with regard to the Fe(III) to Fe(II) conversion, has been claimed to be achieved on gold (7–9), carbon black (10), carbon paste (11–13), spectrographic graphite (14), graphite and Pt (15), pyrolytic graphite (16), and HRP–graphite–epoxy biocomposite (17) by amperometric techniques. Some direct eT reactions with efficient transfer velocity have been detected by relatively fast techniques, such as cyclic voltammetry (8, 9, 16, 17). Schmidt *et al.* (8) investigated the direct eT ability of different biocatalysts, such as HRP, cytochrome *c*, myoglobin, microperoxidase MP-11, and hemin, toward the reduction of H_2O_2 when these proteins were covalently tethered to self-assembled monolayers on gold. Li and Dong (9) further evaluated the direct eT behavior of HRP bound on a 3-mercaptopropionic acid monolayer-modified gold surface by using cyclic voltammetry and electrochemical impedance spectroscopy. Recently, Ferri and co-

[1] To whom correspondence should be addressed. Fax: +86-25-3317761. E-mail: hychen@netra.nju.edu.cn.

[2] Abbreviations used: HRP, horseradish peroxidase; eT, electron transfer; PB, phosphate buffer; ES, enzyme–substrate; Epa, anodic peak potential; Epc, cathodic peak potential; ΔEp, peak-to-peak separation.

0003-2697/00 $35.00

workers (16) studied the direct eT behavior of HRP entrapped within a solid matrix, i.e., a tributylmethylphosphonium chloride polymer-bound anionic exchange resin, at a pyrolytic graphite electrode and used the eT ability to detect H_2O_2.

These enzyme biosensors fabricated with a self-assembly technique can dramatically reduce non-Faradaic background currents and possess high sensitivity and short response time (18, 19). Sometimes, the chemical covalent between the enzymes and the tailed groups immobilized on the electrode surface, however, decreases the bioactivity of enzymes. Although Au nanoparticles as a base for the immobilization of enzymes without loss of their bioactivity have been used to prepare biosensors on a glassy carbon surface (20, 21), to our knowledge the direct eT behavior of HRP immobilized on colloidal Au with a self-assembly technique has not yet been reported. In this paper, we immobilize HRP on 24-nm Au colloid nanoparticles adsorbed on a cysteamine monolayer-modified gold electrode and study the direct eT behavior of immobilized HRP and its electrocatalytic response to the reduction of H_2O_2 by using cyclic voltammetry and chronoamperometry. The immobilized HRP displays a pair of redox peaks (Epa = −96 mV; Epc = −375 mV) in 0.1 M PB (pH 7.0) and can excellently catalyze H_2O_2 reduction, producing a sensitive H_2O_2 sensor. The experimental results indicated that the H_2O_2 sensor can be directly used for determination of H_2O_2 concentration in practical samples with an electrochemical method without the aid of an electron mediator.

MATERIALS AND METHODS

Chemicals and Apparatus

HRP (EC 1.11.1.7, RZ > 3.0, >250 u/mg) and cysteamine were purchased from Sigma. $AuCl_3HCl \cdot 4H_2O$ (Au% > 48%) and all other chemicals were of analytical grade and used without further purification. Phosphate buffer solutions (0.1 M) with various pH values were prepared by mixing stock standard solutions of K_2HPO_4 and KH_2PO_4 and adjusting the pH with 0.1 M H_3PO_4 or NaOH. All solutions were made up with twice-distilled water.

Electrochemical measurements were performed with a three-electrode system comprising a platinum wire as auxiliary electrode, a saturated calomel electrode as reference, against which all potentials were quoted, and the H_2O_2 sensor as working electrode. The electrodes were connected to a BAS-100B electrochemical analyzer with a PA-1 preamplifier (Bioanalytical Systems Inc., U.S.A.). Cyclic voltammetric measurements were done in a thermostated electrochemical cell at 25 ± 0.2°C in a Faraday cage. Amperometric experiments were carried out in a stirred system by applying a potential step of −300 mV to the working electrode. Aliquots of H_2O_2 standard solution were successively added to the solution. Current–time data were recorded after a steady-state current had been achieved. All experimental solutions were deoxygenated by bubbling highly pure nitrogen for 15 min, and a nitrogen atmosphere was kept over the solutions during measurements.

Preparation of Au Colloids

All glassware used in the following procedures were cleaned in a bath of freshly prepared 3:1 HNO_3–HCl and then rinsed thoroughly in twice-distilled water. $HAuCl_4$ and Na_3 citrate aqueous solutions were filtered through a 22-μm microporous membrane filter prior to use. Au colloid was prepared according to the literature (22) by adding Na_3 citrate solution to a boiling $HAuCl_4$ solution. The preparation was stored in dark glass bottles at 4°C. The molar ratio of $HAuCl_4/Na_3$ citrate used for the preparation of the colloid was 0.75. The diameter of the Au colloid was 24 ± 2.1 nm, which was measured using transmission electron microscopy.

Electrode Modification

Gold electrodes were prepared by sealing polycrystalline gold wires (>99.99%, 0.5 mm diameter) in soft glass tubes. The electrodes were abraded with successively finer grades of SiC papers and polished to a mirror-like surface with 0.3- and 0.05-μm alumina slurries on microcloth pads (Buehler), followed by rinsing with water and ethanol and sonicating in twice-distilled water. A roughness factor of 1.4 ± 0.2 was calculated from the ratio of the real to the geometric area (23).

The cleaned gold electrode was first soaked in 20 mM deoxygenated cysteamine aqueous solution for 8 h at room temperature in darkness. The resulting monolayer-modified electrode was thoroughly rinsed with water to remove physically adsorbed cysteamine. Then, it was immersed in an Au colloid solution for 10 h at 4°C. Finally, the Au colloid-modified electrode was incubated in 5 mg/ml HRP PB (pH 7.8) for 12 h to attach HRP molecules to the electrode surface. Thus, the H_2O_2 sensor was obtained. The association of HRP to the colloid surface is possibly due to the interaction between cysteine or NH_3^+–lysine residues of HRP and the Au colloid surface. The preparation process of the H_2O_2 sensor is shown in Scheme 1. All resulting electrodes were washed with water and stored in pH 7.0 PB at 4°C when not in use.

RESULTS AND DISCUSSION

Electrochemical Properties of HRP Immobilized on Colloidal Au Associated with a Cysteamine Monolayer-Modified Gold Electrode

Doron and co-workers (24) reported that small-sized Au colloids can generate continuous arrays of Au par-

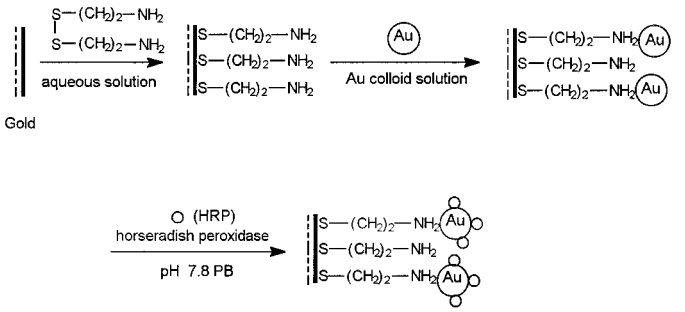

SCHEME 1. Preparation process of the HRP/Au colloid/cysteamine-modified electrode.

ticles on the base monolayers, while the large-sized Au colloids form discontinuous assemblies of nanoparticles on the primary monolayers. Thus, the monolayer associated with the small-sized Au colloid film was more densely packed than the monolayer bound to the large-sized colloids. In previous work (25), we immobilized HRP on different-sized Au colloids attached by a long "cysteamine/glutaraldehyde/cysteamine" molecular bridge at the gold electrode and revealed that HRP molecules bound on the smaller-sized colloids were more abundant than those immobilized on the larger-sized colloids, producing a higher electrocatalytic response. Although the immobilization procedure forms the catalytically active HRP layer on the electrode surface, the average distance between the cofactor and the electrode was too far to achieve the efficiently shuttle processes. This work immobilizes directly HRP to a short Au colloid/cysteamine chain at the gold electrode. The immobilization greatly reduces the direct eT distance between the cofactor and the electrode surface. The small-sized Au colloid (24 nm) associated on the cysteamine monolayer can provide more binding sites than larger-sized colloidal Au (42 nm) for the immobilization of HRP and results in a higher catalytic response to the reduction of H_2O_2. Thus, 24-nm colloidal Au is chosen as the immobilized matrix of HRP molecules.

Figure 1 shows the cyclic voltammograms of Au colloid/cysteamine- and HRP/Au colloid/cysteamine-modified gold electrodes in pH 7.0 PB at 20 mV/s. The irreversible oxidization peak at +275 mV is attributed to the oxidation of colloidal Au attached to the cysteamine monolayer. The HRP/Au colloid/cysteamine-modified electrode displays another pair of redox peaks at −96 mV for Epa and −375 mV for Epc. These peaks result from the redox process of HRP immobilized on colloidal Au film. The direct eT reaction between the prosthetic groups of HRP and the electrode surface can be achieved by the favored orientation of HRP molecules and/or the conducting channels of Au colloids. The surface coverage of HRP immobilized on colloidal Au film is 7.6×10^{-10} mol/cm^2 obtained with chrono-

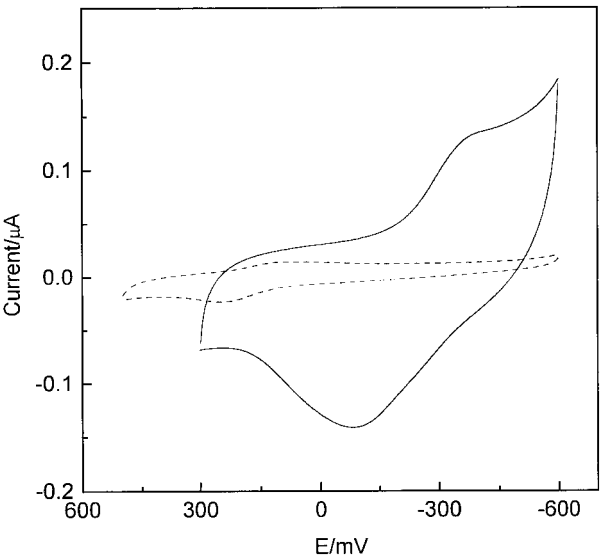

FIG. 1. Cyclic voltammograms of Au colloid/cysteamine (- - -, broken line) and HRP/Au colloid/cysteamine (—, solid line)-modified gold electrodes in pH 7.0 PB at 20 mV/s.

coulometry, which is about 15 times the monolayer coverage of HRP (50 pmol/cm^2) bound to the 3-mercaptopropionic acid monolayer-modified gold surface (9). The amount of HRP attached to the Au colloid film surface was obviously higher than that bound to the organic monolayer.

Figure 2 displays a pair of redox peaks for the direct eT behavior of immobilized HRP at various scan rates.

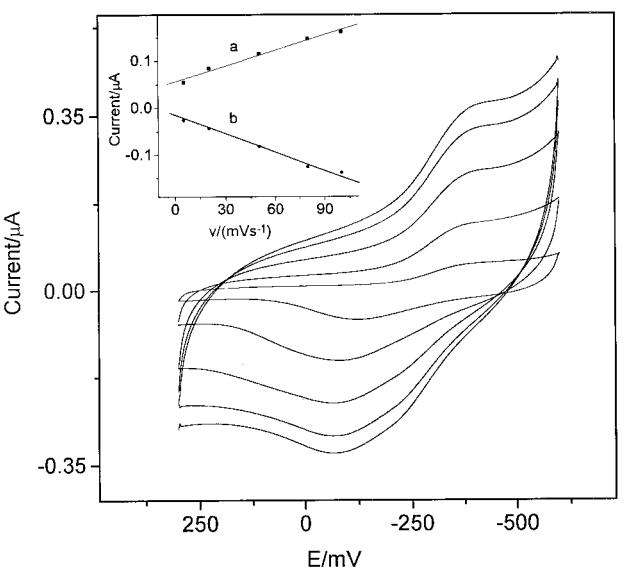

FIG. 2. Cyclic voltammograms of the HRP/Au colloid/cysteamine-modified electrode in pH 7.0 PB at 5, 20, 50, 80, and 100 mV/s. (Inset) Plot of cathodic peak current (a) and anodic peak current (b) vs scan rate.

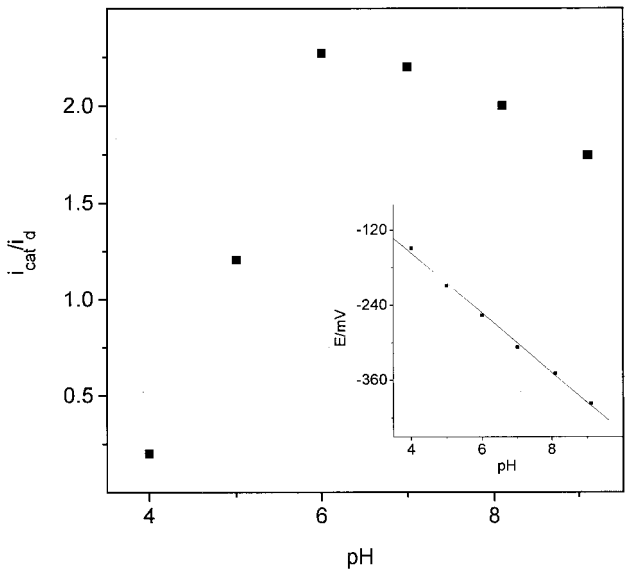

FIG. 3. Effect of pH on the amperometric response (i_{cat}/i_d) at the HRP/Au colloid/cysteamine-modified electrode in PB with various pH values in the presence of 0.19 mM H_2O_2. (Inset) Plot of cathodic peak potential vs pH.

The ratio of cathodic to anodic peak currents is near unity. Peak currents vary linearly with the scan rate, as shown in the inset to Fig. 2, indicating an electrode process as expected for an immobilized system. The cathodic and anodic peak potentials shift very slightly in opposite directions with a change of scan rate. The peak-to-peak separation is 279 mV at 20 mV/s, which is similar to those obtained by other entrapped systems (16, 26). The larger ΔEp is probably ascribable to the immobilized HRP molecules in various orientations (9).

Here the direct electrochemistry of HRP immobilized on colloidal Au is further studied in a pH range of 4.0–9.0 by means of its electrocatalytic behavior to the reduction of H_2O_2 (Fig. 3). At an acidic pH the biocatalytic reaction is diminished due to the denaturation of immobilized HRP. The ratio of i_{cat}/i_d [where i_d and i_{cat} are the cathodic steady-state current before and after adding H_2O_2, respectively (i_{cat}/i_d is used to quantify the electrocatalytic efficiency of HRP to the H_2O_2 reduction)] exhibits a maximum value between pH 6.0 and 7.0, which is in good agreement with that reported for soluble HRP (27). Thus, the Au colloid matrix did not change the optimal pH value for the biocatalytic reaction of immobilized HRP to H_2O_2. A pH value of 7.0 was selected for this study. At the HRP/Au colloid/cysteamine-modified electrode, the cathodic and anodic potentials negatively shifted with increasing pH. The plots of Epc and Epa versus pH gave straight lines with slopes of −49 and −48 mV/pH, respectively. Also, the electron transfer number of heme–iron of HRP is 1; thus, the number of proton ions participating in the redox process was 1.

Figure 4 shows the relationship between peak currents and experimental temperature. The cathodic and anodic peak currents gradually increase with increasing temperature in the range of 13–51°C. When the temperature is higher than 37°C, the change of peak current becomes larger. Experimental results indicated that the bioactivity of HRP could be retained at 51°C for about 3 h.

Electrocatalytic Behaviors of HRP Immobilized on the Au Colloid/Cysteamine-Modified Electrode

Reports in the literature (28, 29) described the direct contact between uncoated, nanometer-sized colloidal Au particles and proteins, where it has been manifested that electrostatically bound colloidal Au:protein conjugates typically retain biological activity. Natan and co-workers (30) observed this property in the study of direct electrochemistry of horse heart cytochrome *c* at SnO_2 electrodes modified with 12-nm-diameter colloidal Au particles and considered that these small Au particles as "electron antennae" could efficiently tunnel electrons between the electrode and the electrolyte. Crumbliss and co-workers (20, 21) prepared the sensors based on the enzyme-covered nanoparticles electrodeposited on a glassy carbon surface. They believed that the small-sized colloidal Au (approximately 30 nm) gave the protein molecules more freedom in orientation and thus increased the possibility that the cofactor of the enzyme approached the metal particle surface, reduced the insulating property of the protein

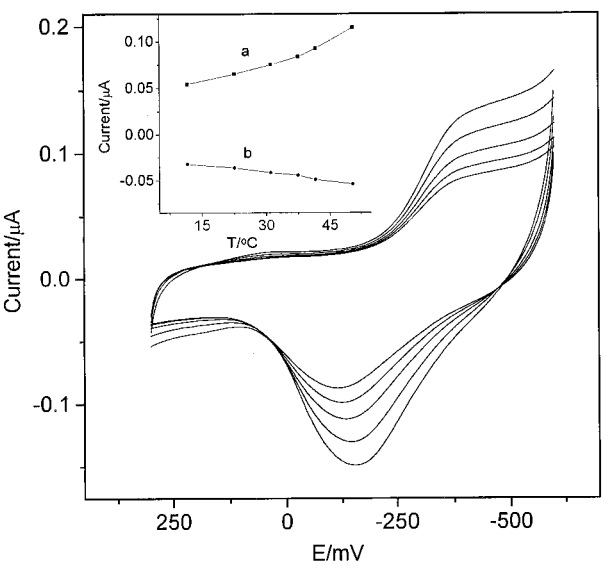

FIG. 4. Cyclic voltammograms of the HRP/Au colloid/cysteamine-modified electrode in pH 7.0 PB at 12, 23, 31, 42, and 51°C (from lowest to highest peak currents). Scan rate, 10 mV/s. (Inset) Plot of cathodic peak current (a) and anodic peak current (b) vs experimental temperature.

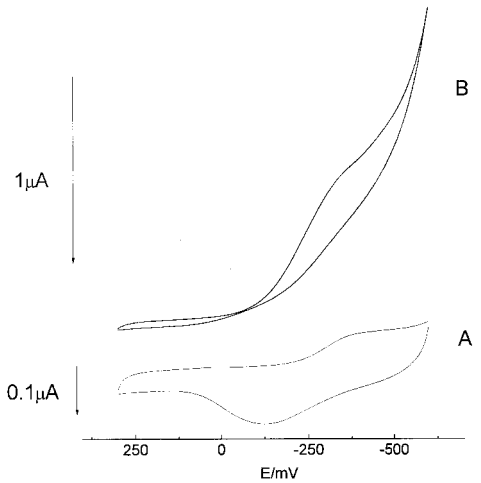

FIG. 5. Cyclic voltammograms of the HRP/Au colloid/cysteamine-modified electrode in pH 7.0 PB at 10 mV/s in the absence of H_2O_2 (A) and in the presence of 9.2 mM H_2O_2 (B).

shell for the direct eT reaction, and facilitated the electron transfer through the conducting tunnels of colloidal Au.

Generally, the electrochemical reduction of the oxidized states of immobilized HRP to the native protein is assumed to be too slow for the cyclic voltammetric technique (2). The rate constant of the direct electrochemical communication is governed by the potential difference of the involved redox centers, by the reorganization energy, and most significantly by the distance between the active site of the enzyme and the electrode surface (9). In the present stage, colloidal Au is attached by the short cysteamine monolayer on the gold electrode surface. Thus, the strong interaction between colloidal Au and HRP may cause adsorbed protein to possess multiple orientations on the colloidal Au surface. Some of the restricted orientations may favor the direct eT reaction due to the short distance between the cofactor of HRP and the electrode surface. The immobilized HRP undertakes a direct eT reaction and exhibits an excellent electrocatalytic response to the reduction of H_2O_2 in pH 7.0 PB. An obvious increase in the cathodic peak current and a complete disappearance in the anodic peak current were observed when 9.2 mM H_2O_2 was added to PB (Fig. 5), indicating that a fast direct eT reaction between the heme site of immobilized HRP and the electrode surface was achieved with a favored orientation of the cofactor toward the electrode surface and/or an efficient electron-conducting tunnel of Au colloid. According to Ref. (16), HRP in this case reacts with H_2O_2 to form a first intermediate (Compound I), which is a two-equivalent oxidized form containing oxyferryl heme (Fe^{4+}═O) and a porphyrin π cation radical. Compound I has catalytic activity and its porphyrin radical abstracts one electron from the electrode to form a second intermediate (Compound II), which is subsequently reduced back to the native HRP by accepting one electron from the electrode. The catalytic mechanism of immobilized HRP to H_2O_2 reduction was exemplified by the following schemes (16):

$$\text{HRP } (Fe^{3+}) + H_2O_2 \rightarrow \text{Compound I } (Fe^{4+}{=}O) + H_2O$$

$$\text{Compound I } (Fe^{4+}{=}O) + e + H^+ \rightarrow \text{Compound II}$$

$$\text{Compound II} + e + H^+ \rightarrow \text{HRP } (Fe^{3+}) + H_2O$$

Also Compound II shows higher stability than Compound I; thus, the reduction process of Compound II to native HRP is slow (9, 16). We can conclude that the one-electron reduction process of Compound II is detected in this experiment.

Determination of H_2O_2 and Apparent Michaelis–Menten Constant

The dependence of the ratio of i_{cat}/i_d on the applied voltage at the HRP/Au colloid/cysteamine-modified electrode is shown in Fig. 6. The ratio of i_{cat}/i_d gradually increases with decreasing negatively applied voltage from −50 to −300 mV and exhibits a maximum value at −300 mV, indicating that the more negatively applied voltage facilitates the reduction of Compound I to HRP (via Compound II). However, i_{cat}/i_d rapidly decreases when the applied voltage is higher than −300 mV. We chose a working voltage of −300 mV for the amperometric determination of H_2O_2, where the risk for interfering reactions of oxygen and other electroac-

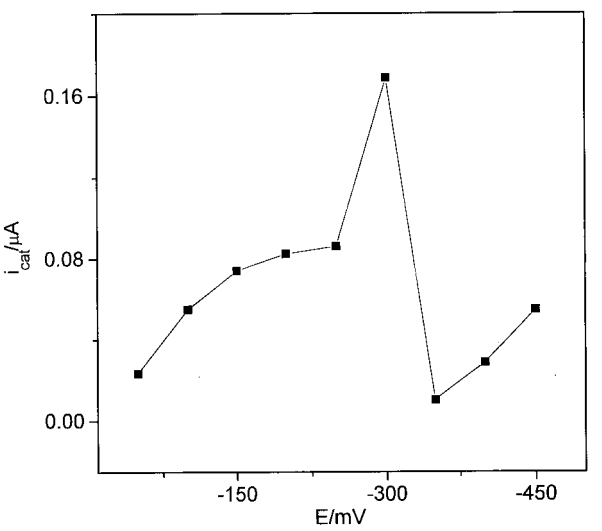

FIG. 6. Dependence of the ratio (i_{cat}/i_d) on applied voltage at the H_2O_2 sensor in pH 7.0 PB in the presence of 0.19 mM H_2O_2.

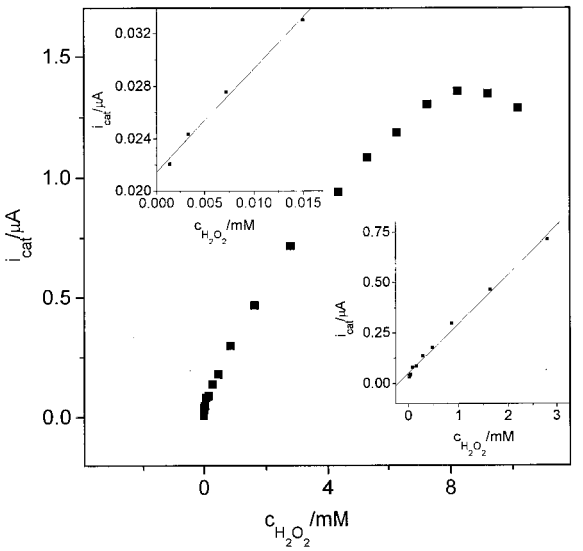

FIG. 7. Amperometric responses of the HRP/Au colloid/cysteamine-modified electrode for successive additions of H_2O_2 in pH 7.0 PB. Insets show linear calibration curves.

tive substances in the solution was minimized and also where the background current and noise levels reached their lowest values.

The chronoamperometric responses of the HRP/Au colloid/cysteamine-modified electrode with successive additions of H_2O_2 are shown in Fig. 7. A considerably fast electrocatalytic response is obtained, with 95% of steady-state current being achieved in less than 15 s, for the H_2O_2 concentration of 9.2 mM. The calibration range of H_2O_2 is 1.4 μM to 9.2 mM with a linear relation from 1.4 μM to 2.8 mM ($R = 0.998$; $n = 17$). The detection limit was estimated to be 0.58 μM at a signal-to-noise ratio of 3. The sensor showed good reproducibility for the determination of H_2O_2 concentration in the linear range. The variation coefficients were 3.1 and 3.9% for 10 successive assays at H_2O_2 concentrations of 46 μM and 2.8 mM, respectively. The fabrication reproducibility of three electrodes, prepared independently, showed an acceptable reproducibility with a variation coefficient of 4.2% for the current determined at 0.47 mM H_2O_2. By the calibration curve method, the recovery experiment of six H_2O_2 samples was performed. The average recovery of the H_2O_2 sensor was 91%.

When the concentration of H_2O_2 was higher than 10 mM, a plateau was observed, showing a characteristic of the Michaelis–Menten kinetic mechanism. The apparent Michaelis–Menten constant (K_m^{app}) is a reflection of both the enzymatic affinity and the ratio of microscopic kinetic constants. It can be obtained from the electrochemical version of the Lineweaver–Burk equation (31):

$$\frac{1}{I_{ss}} = \frac{1}{I_{max}} + \frac{K_M^{app}}{I_{max}C}.$$

Here, I_{ss} is the steady-state current after the addition of substrate, C is the bulk concentration of the substrate, and I_{max} is the maximum current measured under saturated substrate conditions. Also, $K_M^{app} = (k_{-1} + k_2/k_1)$ is the ratio of the rates of breakdown of ES to its rate of formation. Usually, k_{-1} is much greater than k_2 for many enzymes (32); thus, K_m^{app} becomes a measure of the affinity of an enzyme for its substrate since its value depends on the relative values of k_1 and k_{-1} for ES formation and dissociation, respectively (32). A low K_m^{app} value indicates strong substrate binding. The K_m^{app} value for the HRP/Au colloid/cysteamine-modified electrode was found to be 2.3 mM. This value was lower than that reported (16), giving clear evidence for the higher sensitivity of the HRP/Au colloid/cysteamine-modified electrode. However, the K_m^{app} value was markedly higher than that obtained for HRP immobilized on the long "Au colloid/cysteamine/glutaraldehyde/cysteamine" molecular bridge at the gold electrode surface (25), in which the K_m^{app} value was 0.094 mM. These results indicate that HRP molecules immobilized on the short "Au colloid/cysteamine monolayer" chain may partially adsorb on the bulk gold electrode surface and decrease its affinity for H_2O_2.

Stability of the HRP/Au Colloid/Cysteamine-Modified Electrode

The stability of the HRP/Au colloid/cysteamine-modified electrode was studied in the linear range of H_2O_2. When the H_2O_2 sensor was stored in a pH 7.0 PB for at least 2 weeks at 4°C, the sensor retained >87% of its initial sensitivity to the reduction of H_2O_2. The deterioration of the sensor may be due to the deactivation of immobilized HRP. When the concentration of H_2O_2 was higher than 10 mM, denaturation of HRP occurred, and the HRP was irreversibly transformed into its higher oxidized, inactive form (Compound III) (33). Thus, high concentrations of H_2O_2 should be avoided in order to maintain the bioactivity of HRP over a longer period of time.

ACKNOWLEDGMENTS

This project was supported by the National Natural Science Foundation of China (Grant 29835110). Ju H.-X. acknowledges financial support from the Scientific Research Foundation for Returned Overseas Chinese Scholars, the Ministry of Education of China, and the Natural Science Foundation of Jiangsu.

REFERENCES

1. Santucci, R., Picciau, A., Campanella, L., and Brunori, M. (1994) *Curr. Top. Electrochem.* **3,** 313–328.

2. Ruzgas, T., Csoregi, E., Emneus, J., Gorton, L., and Marko-Varga, G. (1996) *Anal. Chim. Acta* **330,** 123–138.
3. Tatsuma, T., Okawa, Y., and Watanabe, T. (1989) *Anal. Chem.* **61,** 2352–2355.
4. Garguilo, M. G., Huynh, N., Proctor, A., and Michael, A. C. (1993) *Anal. Chem.* **65,** 523–528.
5. Kulys, J. J. (1986) *Biosensors* **3,** 3.
6. Bartlett, P. N., Tebbutt, P., and Whitaker, R. G. (1991) *Prog. React. Kinet.* **16,** 55.
7. Razumas, V. J., Gudavicius, A. V., and Kulys, J. J. (1983) *J. Electroanal. Chem.* **151,** 311–315.
8. Lötzbeyer, T., Schuhmann, W., and Schmidt, H.-L. (1997) *Bioelectrochem. Bioenerg.* **42,** 1–6.
9. Li, J., and Dong, S. (1997) *J. Electroanal. Chem.* **431,** 19–22.
10. Yaropolov, A. I., Malovik, V., Varfolomeev, S. D., and Berezin, I. V. (1979) *Dokl. Akad. Nauk SSSR* **249,** 1399.
11. Gorton, L., Jönsson-Pettersson, G., Csöregi, E., Johansson, K., Domínguez, E., and Marko-Varga, G. (1992) *Analyst* **117,** 1235–1241.
12. Gorton, L., Csöregi, E., Domínguez, E., Emnéus, J., Jönsson-Pettersson, G., Marko-Varga, G., and Persson, B. (1991) *Anal. Chim. Acta* **250,** 203–248.
13. Chut, S. L., Li, J., and Tan, S. N. (1997) *Analyst* **122,** 1431–1434.
14. Jönsson-Pettersson, G., and Gorton, L. (1989) *Electroanalysis* **1,** 465–468.
15. Wollenberger, U., Bogdanovskaya, V., Bobrin, S., Scheller, F., and Tarasevich, M. (1990) *Anal. Lett.* **23,** 1795–1808.
16. Ferri, T., Poscia, A., and Santucci, R. (1998) *Bioelectrochem. Bioenerg.* **44,** 177–181; **45,** 221–226.
17. Morales, A., Céspedes, F., Muñoz, J., Martínez-Fàbregas, E., and Alegret, S. (1996) *Anal. Chim. Acta* **332,** 131–138.
18. Willner, I., Lapidot, N., Riklin, A., Kasher, R., Zahavy, E., and Katz, E. (1994) *J. Am. Chem. Soc.* **116,** 1428–1441.
19. Riklin, A., and Willner, I. (1995) *Anal. Chem.* **67,** 4118–4126.
20. Zhao, J., Stonchuerner, R. W., O'Daly, J. P., and Crumbliss, A. L. (1992) *J. Electroanal. Chem.* **327,** 109–119.
21. Crumbliss, A. L., Stonchuerner, J. G., Henkens, R. W., Zhao, J., and O'Daly, J. P. (1993) *Biosens. Bioelectron.* **8,** 331.
22. Turkevich, J., Stevenson, P. C., and Hillier, J. (1951) *Discuss. Faraday Soc.* **11,** 55–75.
23. Oesch, U., and Janata, J. (1983) *Electrochim. Acta* **28,** 1237–1246.
24. Doron, A., Katz, E., and Willner, I. (1995) *Langmuir* **11,** 1313–1317.
25. Xiao, Y., Ju, H. X., and Chen, H. Y. (1999) *Anal. Chim. Acta* **391,** 73–82.
26. Murray, R. W. (1984) *in* Electroanalytical Chemistry (Bard, J. A., Ed.), Vol. 13, pp. 205, Dekker, New York.
27. Harbury, H. A. (1957) *J. Biol. Chem.* **225,** 1009.
28. Geoghegan, W. D., and Ackerman, G. A. (1977) *J. Histochem. Cytochem.* **25,** 1187–1200.
29. Horisberger, M. (1983) *Trends Biochem. Sci.* **8,** 395.
30. Brown, K. R., Fox, A. P., and Natan, M. J. (1996) *J. Am. Chem. Soc.* **118,** 1154–1157.
31. Kamin, R. A., and Willson, G. S. (1980) *Anal. Chem.* **52,** 1198–1205.
32. Hames, B. D., Hooper, N. M., and Houghton, J. D. (1997) *in* Instant Notes in Biochemistry, p. 67.
33. Aderian, S. A., and Lambeir, A. M. (1989) *Eur. J. Biochem.* **186,** 571.